ISTITUTO NAZIONALE DI FISICA NUCLEARE - ISTITUTO NAZIONALE DI FISICA NUCLEARE - ISTITUTO NAZIONALE DI FISICA NUCLEARE - ISTITUTO NAZIONALE DI FISICA NUCLEARE - ISTITUTO NAZIONALE DI FISICA NUCLEARE - ISTITUTO NAZIONALE DI

Laboratori Nazionali di Frascati

LNF-93/055 (R)
10 Settembre 1993

WIZARD - MASS Collaboration

Papers presented at the XXIII International Cosmic Rays Conference, Calgary 1993

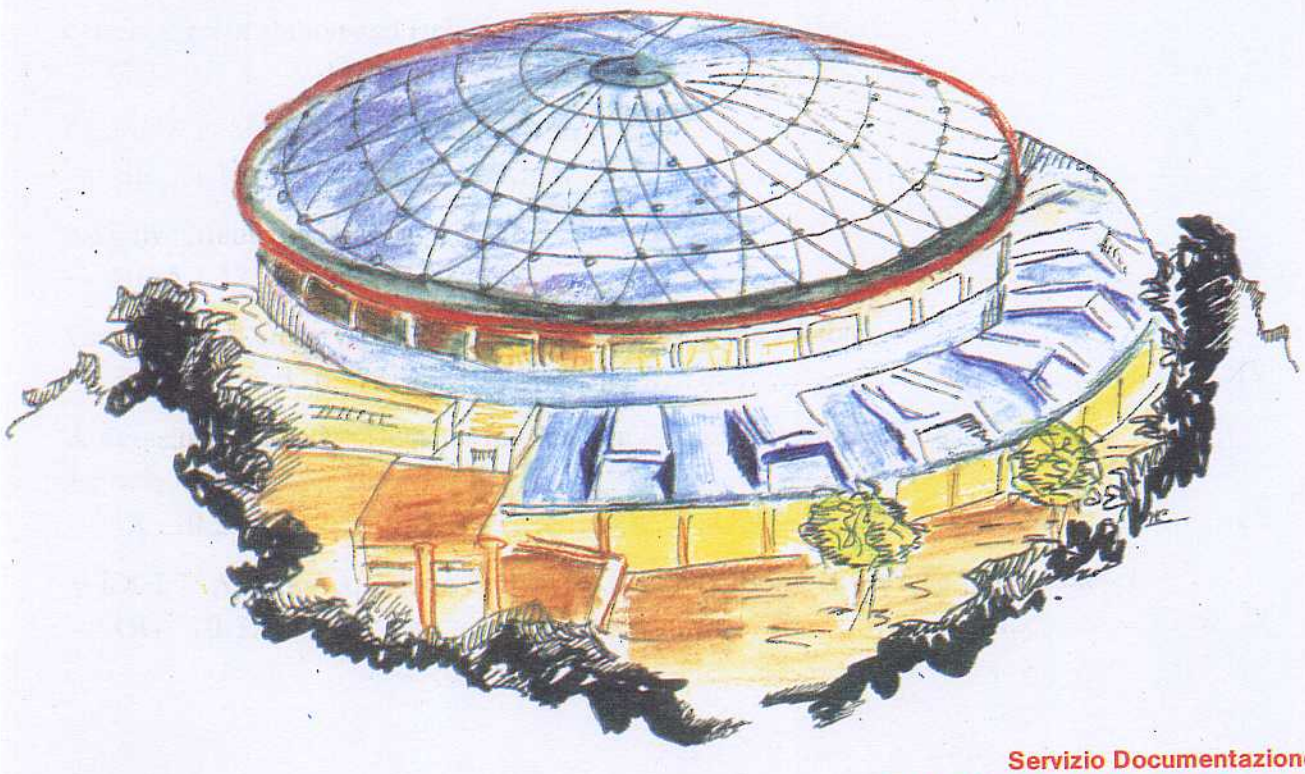

Servizio Documentazione
dei Laboratori Nazionali di Frascati
P.O. Box, 13 - 00044 Frascati (Italy)

INFN - Laboratori Nazionali di Frascati
Servizio Documentazione

LNF-93/055 (R)
10 Settembre 1993

WIZARD - MASS Collaboration

Papers presented at the XXIII International Cosmic Rays Conference, Calgary 1993

CONTENTS

Calgary 1993 XXIII ICRC OG 10.3.7 v.2

A Silicon Shower Detector For Cosmic Antimatter Search

F. Aversa[1], G. Barbiellini[2], G. Basini[3], P. Battaiotto[2], V. Bidoli[4], M. Bocciolini[5], M. Boezio[2], F. Bongiorno[3], F. Bronzini[7], M.T. Brunetti[6], M. Candusso[4], G. Cantatore[2], M. Casolino[4], F. Celletti[5], A. Codino[6], A. Colavita[1], M.P. De Pascale[4], F. Fratnik[2], M. Grandi[5], C. Grimani[6], F. Massimo Brancaccio[3], G. Mazzenga[3], M. Menichelli[6], M. Miozza[6], A. Morselli[4], A. Perego[5], P. Picozza[4], M. Ricci[3], I. Salvatori[4], P. Schiavon[2], P. Spillantini[5], A. Vacchi[2], N. Zampa[2]

1. INFN / ICTP-Microprocessor Laboratory, Trieste, Italy 2. Dipartimento di Fisica dell' Università and INFN, Trieste, Italy 3. INFN-Laboratori Nazionali di Frascati, Italy 4. Dipartimento di Fisica dell' Università and INFN, Roma-Tor Vergata, Italy 5.Dipartimento di Fisica dell' Università and INFN, Firenze, Italy 6.Dipartimento di Fisica dell' Università and INFN, Perugia, Italy 7. Dipartimento di Fisica dell' Università and INFN, Roma, Italy

ABSTRACT

We describe a silicon sampling shower detector conceived as a fine grain imaging device to carry out studies on the anitmatter component in the cosmic radiation. This instrument, that will be flown during the 1993 balloon flight campaign, is formed by 5 xy sensitive layers (strip pitch 3.6 mm) interleaved with 4 showering material planes (tungsten 1 radiation length) having low power consumption electronic readout.

1. INTRODUCTION

A silicon tungsten (SiW) detector[1,2] has been built and tested in order to provide complementary informations for the identification of high energy positrons and electrons to study the e^+/e^- ratio up to 50 GeV. This study aims at the determination of the production and propagation mechanism of antimatter in the primary cosmic radiation. The detector is installed in the NASA-Balloon Borne Magnet Facility[3,4] (BBMF) and contains a total of 5 xy silicon sampling layers and 4 radiation lengths of tungsten.

This device is due to add two orders of magnitude in hadron rejection power to the rest of the spectrometer which is composed of a Transition Radiation Detector[5] (TRD) and a magnetic spectrometer with Drift and MultiWire Proportional Chambers (MWPC.)

For the 1993 flight of the BBMF the spectrometer has been prepared to study the positron spectrum in the 4 - 50 GeV energy range. The positron/proton ratio in the primary cosmic radiation is of the order of 10^{-3} at low energies decreasing towards higher energies. A reliable measurement of positrons requires a rejection power against protons of the order of 10^{-5} or better. This can be achieved through the joint performance of the TRD and the SiW shower detector. The silicon tungsten detector acts as the high granularity track and shower imaging device. Being sensitive to minimun ionizing particles, it allows to follow the tracks of nonelectromagnetic interacting particles by measuring the ionization energy left. It also allows to measure the shape and the energy left by developing showers as well as the shower starting point and the direction of the originating particle. This device is very compact and allows to improve significantly the geometric factor of the experiment.

Futhermore, in view of a foreseen series of long duration flights this instrument (which will be upgraded to contain at least 15 xy silicon detector layers) will allow the thorough testing of the complete detector and the electronic system for future space applications.

2. DESCRIPTION OF THE DETECTOR

Being conceived for present balloon borne experiments and for future space applications, such a device has to satisfy specific requirements of low weigth, minimal

power consumption and high reliability. Furthermore, the geometrical parameters of the detector (like the distance between the sensitives planes) are affected by the structural constraints imposed by the stresses occurring during the different phases of the flight.

The complete device, whose characteristics are reported in Table 1, consists of 5 xy layers of silicon detectors alternated with 4 planes of tungsten. A single layer is composed as a 8•8 matrix of sensitive modules to obtain a total of 256 readout channels.

TABLE 1
Detector characteristics

Total sensitive area	(492 • 492) mm^2
Single detector dead area (guards, edges)	5%
Assembled plane total dead area	10%
Thickness of the Si-D per sampling	2 • 380 (or 300)μm
Single detector area	(60 • 60) mm^2
Number of detectors per plane (x and y)	(8 •8) • 2 = 128
Pitch of the strips on the Si-D (16 strips)	3.6 mm
Mean leakage current	10 nA cm^{-2}
Working voltage (>full depletion)	≤120 V
Crystal n-type (FZ) resistivity	≥ 4 kΩ cm
Readout coupling	ohmic
Strip capacitance (full depletion)	~70 pF
Number of electronic channels per plane	256
Front-end power dissipation per channel	20 mW
Total input capacitance to the preamplifier	~ 560 pF
Mean electronic noise (7μs shaping time)	3500 ENC
Thickness of the tungsten plates	3.50 mm (1.0 X_0)
Total depth (W)	4.0 X_0
Total thickness	7.5 cm

One sensitive module is composed of two Si detectors[6], each having a total area of (60×60) mm^2 and a thickness of 380μm (or 300μm according to different types of Si detectors); they are mounted back to back with an on-line pin structure and perpendicular strips to give *x* and *y* coordinates. Each detector has 16 strips 3.6 mm wide. In our application the detectors are hold in a special package which, when patched to form large surfaces, allows a minimal dead area for the sampling planes.

The packaged silicon detectors are assembled on a multilayer board, which also carries the front-end electronics and the related wiring. The strips of each detector are connected to the neighbouring one to form single strips 50 cm long.

The design of a dedicated front-end electronics has been carried out in order to satisfy the above mentioned requirements for space applications. The preamplifiers[7] are grouped in 16-channel modules that convert the charge signals coming from the 16 strips of each silicon detector. The shaping time (7μs) has been designed in order to optimize the signal-to-noise ratio. Digital control inputs perform the routing of 16 levels onto a single output during the readout operations by means of a sample-and-hold and multiplexing procedure. Two full-scale outputs are available to give a linear response up to 25 or 400 minimum ionizing particles (mip) in order to cover the very large dynamic range required in the detector.

The whole data acquisition system has been integrated in the detector; it receives analog signals from the hybrid preamplifier modules, controls the digitization of the signals and performs a pedestal and zero suppression analisys providing the resulting information to the fligth control computer. A modular architecture was chosen that could support up to 32 detector planes and servicing 40-80 events per second. This goal is attained by assigning a Digital Signal Processor (DSP) to service all the functions of each plane. All DSPs are controlled by a master computer (GMX) that performs the execution of housekeeping tasks such as pedestal measurements, calculation of zero suppression thresholds and preamplifier linearity tests. One DSP per plane controls the conversion procedure of 16 ADC converter chips residing on each plane and broadcasts all instructions to the ADC since all of them perform the

same tasks in parallel. The data contained in the ADC FIFO's are individually read by the DSP that compares the digitized voltage with a threshold value. There is a threshold value for each and all the channels in the plane. The DSP sends the converted signals above threshold to the GMX together with the position of the channel that generated the signal and the amplification used. The whole readout time of a single event is about 3.5 msec. The GMX writes the data on a dual port memory located in a CAMAC crate from which the flight control computer gathers the informations to be sent to ground.

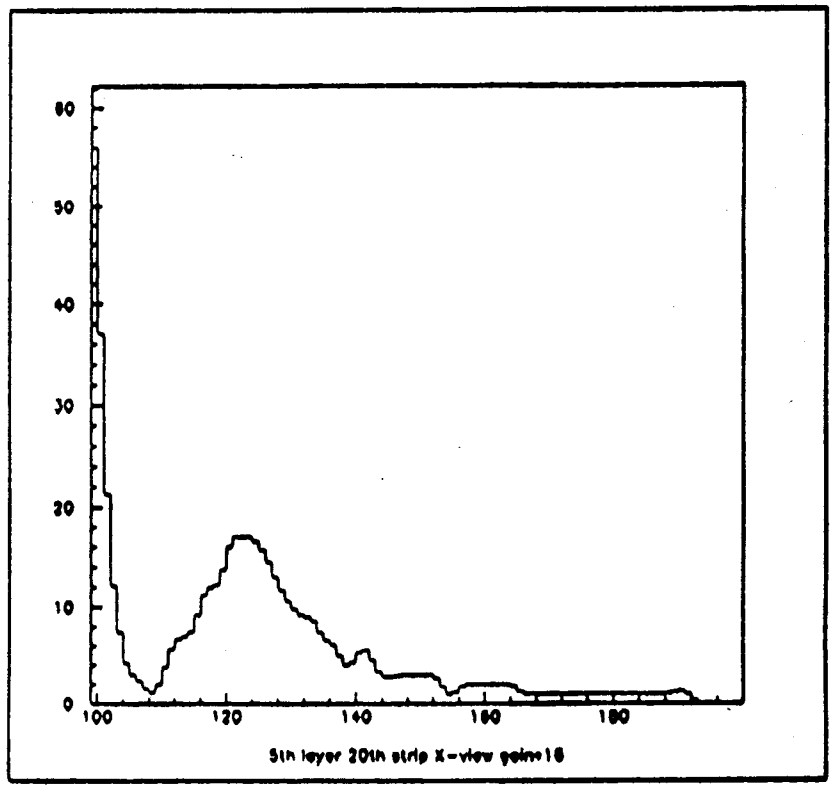

Fig. 1. Pulse height distribution for ground muons detected in one single strip. The residual of the pedestal peak is also shown in the first ADC channels.

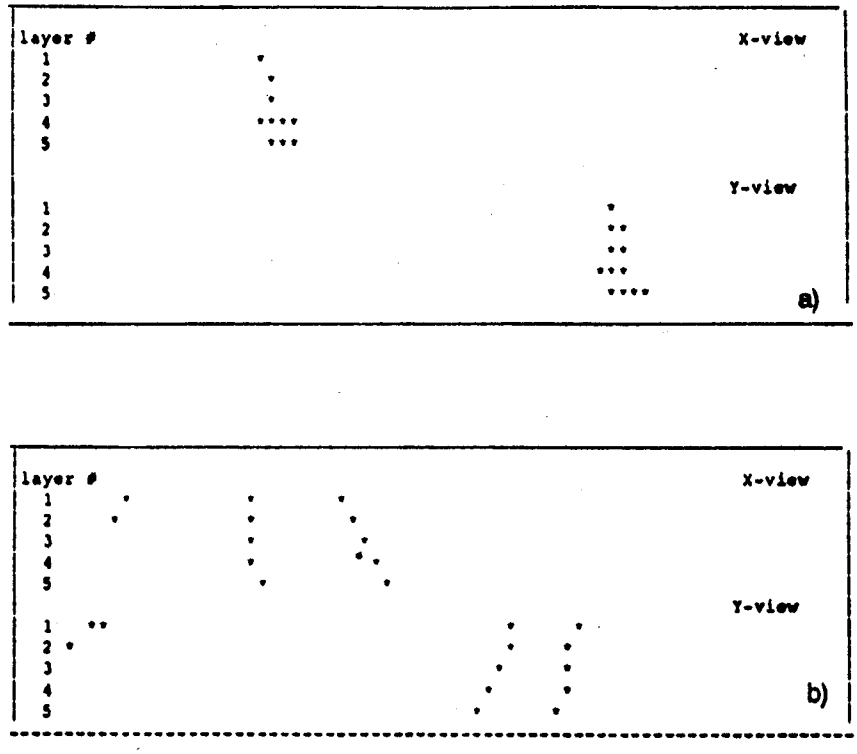

Fig. 2. Representation of ground muon raw data as seen in the silicon shower detector; a) development of an e.m. shower, b) a dimuon event.

3. PERFORMANCES

A complete test of one of the sampling layers was performed at the PS t7 teast beam at CERN. An accurate study of the separation between the noise and the minimun ionizing peak has been carried out using a pion beam at 4 GeV for each strip. Furthermore, using an electron beam at 4 GeV and adding 4 X_0 tungsten layers behind the plane, also second and third ionization peaks were visible.

Preliminary results obtained from ground cosmic ray tests during the detector integration in the BBMF are shown in Figg 1,2. The raw distribution of the muon signal detected in one single strip is visible in Fig. 1 as well as the residual of the pedestal peak; the representation of some events in both x and y views is shown in Fig. 2.

REFERENCES

(1) Barbiellini, G., et al.: 1992, INFN/AE-92/17; also to appear in Nucl.Inst.Meth.
(2) Bocciolini, M., et al.: to appear in Proc.3rd Int. Conf. on Advanced Technology and Particle Physics, 1992, Villa Olmo, Como, Italy
(3) Golden, R.L., et al.: 1991, Nucl. Inst. Meth., A306, 366
(4) Golden, R.L., et al.: 1992,'WiZard-Related Balloon Program", proposal submitted in response to NRA-92-OSSA-10
(5) Bellotti, R., et al.: 1993, these Proceedings
(6) Build by Camberra (Belgium), Hamamatsu (Japan) and SGS (Italy)
(7) Build by LABEN (Italy)

Calgary 1993 XXIII ICRC OG 5.3.1 v.1

Observations of Proton And Helium Spectra Near Solar Maximum.

P. Papini[5],C. Grimani[6],G. Basini[1], F. Bongiorno[1], M. T. Brunetti[6], A. Codino[6], R. L. Golden[2], B. L. Kimbell[2], F. Massimo Brancaccio[1], M. Menichelli[6], M. Miozza[6], A Morselli[3], J.F.Ormes[4], M. P. De Pascale[3], P. Picozza[3], M. Ricci[1], I. Salvatori[6], P. Spillantini[5], S. A. Stephens[2,7], S. J. Stochaj[2], R. E. Streitmatter[4], W. R. Webber[2]

1. INFN-Laboratori Nationali di Frascati, Italy, 2. New Mexico State University, New Mexico, USA 3. Dipartimento di Fisica and INFN dell'Universita' di Roma "Tor Vergata", Italy 4. NASA - Goddard Space Flight Center, Maryland. USA 5. Dipartimento di Fisica and INFN dell'Universita' di Firenze, Italy 6. Dipartimento di Fisica and INFN dell' Universita' di Perugia, Italy 7. Tata Institute of Fundamental Research, Bombay, India 8. Dipartimento di Fisica and INFN dell'Universita' di Roma, Italy.

ABSTRACT

Measurements of the proton and helium spectra were made on September 5th 1989 using the balloon-borne experiment MASS. The instrument was above 10 g/cm^2 for 5.5 hours near Prince Albert, Saskatchewan (Canada). The measured fluxes have been corrected to the top of the atmosphere. At the top of the atmosphere, the kinetic energy range of the observations was 0.117 - 39 GeV/n for protons and 0.171 - 19.97 GeV/n for helium. The measurements have been performed during 1989, very near the maximum of the last solar cycle. On the day of the flight the Mt. Washington Neutron Monitor rate was 1961.

1. INTRODUCTION

Protons and helium nuclei are the main cosmic ray constituents (about 98%). The intensity and energy distributions of these particles, as observed at earth, are known to be modulated by the solar wind. This knowledge was gained primarily by observations made for more than 4 decades of integral count rates above the local geomagnetic cutoff. The advent of magnetic spectrometers has possible to make much more detailed measurements of solar modulation over large energy ranges, by observing differential energy spectra. This paper represents the first step in providing a summary of observations of proton and helium differential energy spectra over the last 17 years. There are spectra from 5 previous flights of this instrument dating back to 1976 which will be reported in a future compendium of our observations. The observations reported here are of special value because this version of the instrument incorporated an imaging calorimeter, which allowed significant improvements in the accuracy to which the observing efficiencies could be determined. The flight reported here also happen to take place during the strongest solar activity experienced during our observing program. The high energy spectra from this flight provides a means of cross-calibrating and cross-checking the intensities and energy spectra observed in the earlier flights.

In this paper we describe the instrument and data analysis briefly in sections 2 and 3. Section 4 contains the results and section 5 provides a summary of the findings.

2. EXPERIMENT

The MASS apparatus consists of a superconducting magnet spectrometer, a scintillator TOF system (T1 -T2 above the spectrometer and T3 - T4 below the spectrometer), a high resolution scintillator (S1), a gas-Cherenkov detector and a streamer tube calorimeter. The magnetic spectrometer which uses multi-wire

proportional chambers (MWPC) is described in Golden et al. (1991). Event read-out is initiated by a coincidence between T1, T2, T3 and T4. Events transmitted to the ground were also required to have an S1 pulse-height greater than 0.25 times that corresponding to a minimum ionizing particle.

The Cherenkov detector was filled with a 50 - 50 mixture of Freon 12 and Freon 22 that has a threshold of Lorentz factor of 23. The calorimeter each consisted of 40 layers of 64 brass streamer tubes. The material in the calorimeter is equivalent to 7.3 radiation lengths and 0.7 nuclear interaction lengths. The calorimeter permits the reconstruction of the topological structure of the particle interactions. More details on the apparatus performance and characteristics are given in De Pascale et al., 1991 and references therein.

3. DATA ANALYSIS

Data analysis has been performed selecting positive particles in the rigidity r (r=p/Zq) interval 0.310 - 40 GV/c (as measured at the magnetic spectrometer) for protons and 1 - 41.7 GV/c for helium. The selection criteria for the MWPC are those given in (Golden et al. 1991). The scintillators T1- T2 - T3 - T4 and the high resolution scintillator S1 were used to determine the charge of each particle. The amplitude of the signal (P) generated by a particle going through a scintillator is related to the particle mass (m), deflection (d) and charge (Z), from the relation:

$$P = (m\,d)^2 + Z^2$$

Therefore it is possible to separate particles with different charge, plotting the scintillator output versus the particle deflection squared. In Fig. 1 shows the separation between particles with charge 1 (protons) and 2 (helium).

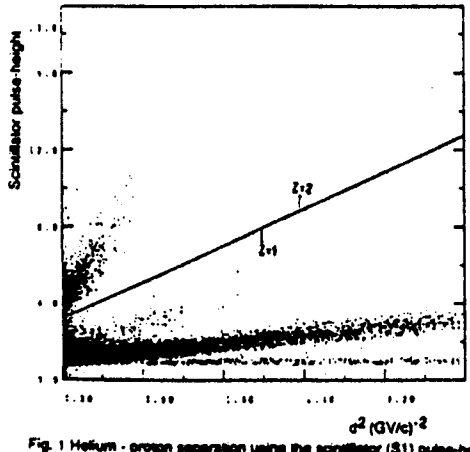

Fig. 1 Helium - proton separation using the scintillator (S1) pulse-height vs deflection squared.

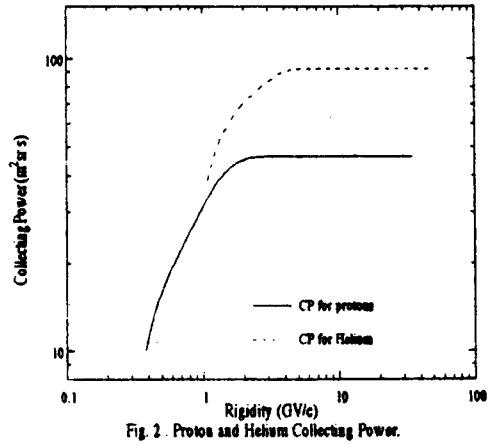

Fig. 2 . Proton and Helium Collecting Power.

4. RESULTS

The proton and helium spectra at the top of the atmosphere have been first obtained calculating the rigidity fluxes at the spectrometer, including the experiment geometrical factor, the efficiencies of the detectors and the total exposure time, then recalculating the fluxes versus kinetic energy and propagating them to the top of the atmosphere. The geometrical factor and the MWPC efficiency are energy dependent. This dependence has been described in detail in De Pascale et al., 1991.

The total elapsed time was 19812 sec., with 33% dead-time due to on-board data processing. Six percent of the data are lost due do computer dead time during transcription of the analog tapes. Since Z=1 particles require the calorimeter and Cherenkov for proper identification, we selected these particles in a

restricted geometry (Basini et al. 1991). The master trigger was cross-checked with smaller trigger paddles on the ground, to make sure the overall geometric factor and sensitivity were determined. The effective efficiency of the master trigger was found to be 0.90. Helium was selected with a less restrictive geometry. The effective trigger efficiency was 0.83. The collecting power for both proton and helium are given in Fig. 2.

The proton rigidity spectrum as measured at the spectrometer (Fig. 3), were corrected to the top of the payload using a multi-step process. The first step was to correct for the ionization energy losses in the detectors located above the spectrometer. Then the secondary proton flux, mainly produced from primary proton interaction in the 5 g/cm^2 of residual atmosphere overlying the payload, was subtracted using the secondary spectra computed by Rygg and Earl, 1971. The Rygg and Earl spectrum was calculated for a Deep River Neutron Monitor rate of 6700, which corresponds to a substantially lower solar modulation than that during the observation reported here. To correct for the differences in modulation strength, the Rygg and Earl spectrum of secondaries was normalized using our observations below the geomagnetic cut-off (650 MV/c).

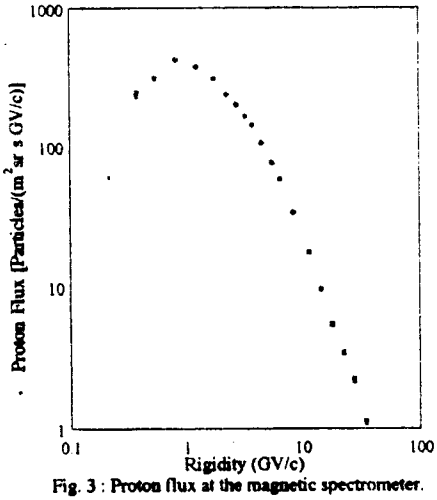

Fig. 3 : Proton flux at the magnetic spectrometer.

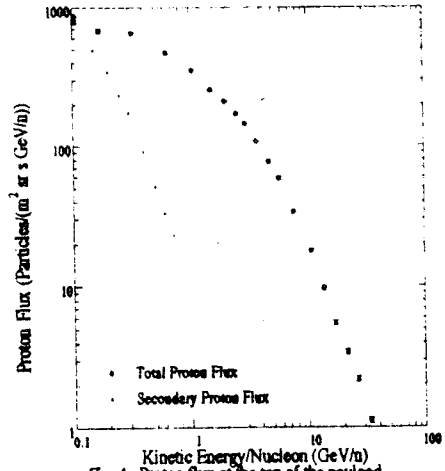

Fig. 4 : Proton flux at the top of the payload with secondary particle contribution shown.

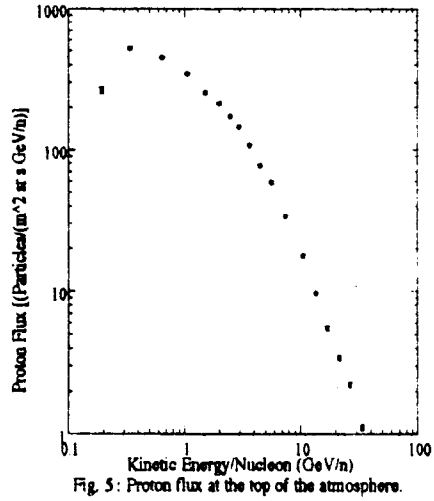

Fig. 5 : Proton flux at the top of the atmosphere.

The contribution of the secondary protons to the total flux at the top of the payload is shown in Fig. 4. The final step was to correct for the ionization energy losses in the atmosphere. In Fig. 5 we show our observed proton spectrum corrected to the top of the atmosphere. Note that the spectra were not corrected for the finite resolution of the momentum spectrometer. As reported in Golden et al. 1991, the maximum detectable rigidity was found to be 118 GV for this observation. This corresponds to nearly a factor of 3 higher rigidity than that reported in this observation.

The helium flux at the spectrometer (Fig. 6) was corrected to the top of the

atmosphere by allowing for the ionization energy losses in the atmosphere and in the payload. Corrections were also made for helium interactions in the payload and atmospheric productions/interactions. The helium flux at the top of the atmosphere is presented in Fig. 7.

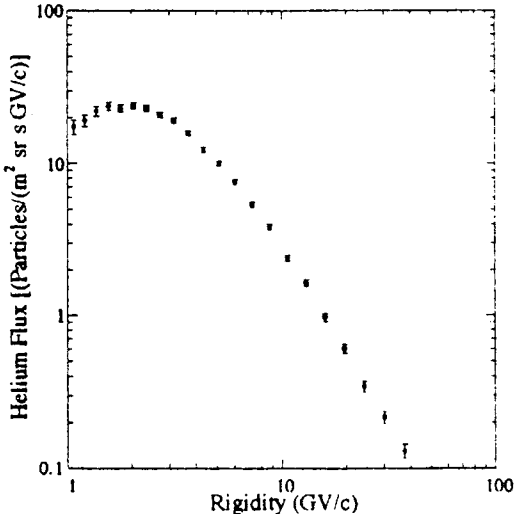

Fig. 6 : Helium flux at the magnetic spectrometer.

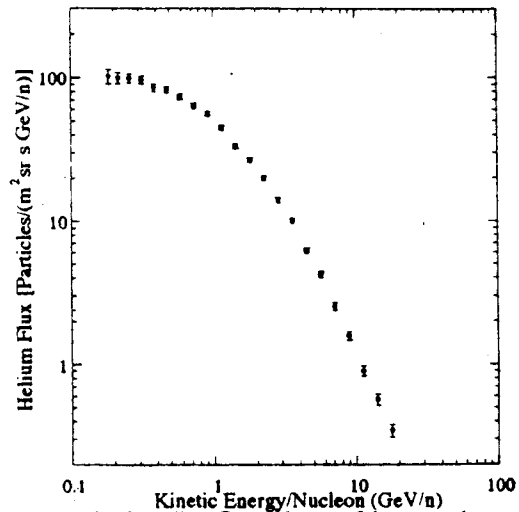

Fig. 7 : Helium flux at the top of the atmosphere.

5. DISCUSSION

Both the proton and helium intensities show extreme depression at lower energies. In comparison to data from previous flights, we find the fluxes reduced by 2-5 times at low energies (less than 10 GeV/n). The proton spectrum at the top of the atmosphere can be represented by a power law in kinetic energy/nucleon with a spectra index of (-2.33±0.03) at energies greater than 10.5 GeV/n. For helium the spectral index is found to be (-2.19±0.17) at energies greater than 8.9 GeV/n. These spectra are very flat compared to the more typical spectral indices of (2.6 - 2.7) reported by previous observations by this group and by others. As a cross-check that the momentum spectrometer was working correctly and properly calibrated, the spectrum of protons accompanied by Cherenkov light, was used to confirm that the threshold rigidity corresponded to a Lorentz factor of 23. It is believed this extraordinary change in spectral index is due to solar modulation. Data from past and future flights of our experiment, carried-out during different periods of solar modulation will give us interesting hints about solar modulation effects on both protons and helium during their propagation to the Earth.

6. ACKNOWLEDGMENT

This work was supported by NASA grant NAG-110, the Istituto Nazionale di Fisica Nucleare, Italy and the Agenzia Spaziale Italiana. A very special thank to our technical support staff from NMSU and INFN.

REFERENCES

Basini, G. et al.:1991, Proc. 22th Internat. Cosmic Ray Conf., Dublin (Ireland), **2**, 137, also submitted to Ap. J..
De Pascale, M.P., et al.,:1993, J. Geophys. Res., **98**(A3), 3501.
Der Verma, S.:1967, J. Geophys. Res., **72**(3), 915.
Golden, R.L. et al.:1991, Nucl. Instr. Meth., **A396**, 366.
Rygg, T.A. and Earl, J.A.:1971, J. Geophys. Res., **76**(31) 7445.
Teegarden, B.J.:1967, J. Geophys. Res., **72**(19), 4857.

Calgary 1993 XXIII ICRC HE 5.1.11 v.4

Cosmic Ray Muon Spectrum in the Atmosphere

M. Circella[1], F. Cafagna[1], G. Basini[2], R. Bellotti[1], F. Bongiorno[2,3], M. T. Brunetti[4], A. Codino[4], C. De Marzo[1], M. P. De Pascale[5], R. L. Golden[6], C. Grimani[4], B. L. Kimbell[6], F. Massimo Brancaccio[2], M. Menichelli[4], A. Morselli[5], J. F. Ormes[7], P. Papini[8], P. Picozza[5], M. Ricci[2], I. Salvatori[4], E. S. Seo[7], P. Spillantini[8], S. A. Stephens[6,9], S. J. Stochaj[6], R. E. Streitmatter[7], and W. R. Webber[6]

[1]Universita' di Bari and INFN, Bari, Italy. [2]INFN, Laboratori Nazionali di Frascati, Italy. [3]Universita' di Roma "La Sapienza" , Rome, Italy. [4]Universita' di Perugia and INFN, Perugia, Italy. [5]Universita' di Roma "Tor Vergata" and INFN, Rome, Italy. [6]Particle Astrophysics Laboratory, New Mexico State University, USA. [7]NASA, Goddard Space Flight Center, Maryland, USA. [8]Universita' di Firenze and INFN, Firenze, Italy. [9]Tata Institute of Fundamental Research, Bombay, India.

ABSTRACT

A measurement of the negative muon flux in the atmosphere has been carried out using the data collected by the Matter-Antimatter Superconducting Spectrometer (MASS) apparatus during the ascent of the 1989 flight. This experiment was flown on September 5, 1989 from Prince Albert, Saskatchewan (Canada). The muon spectrum has been determined in the momentum interval 0.3-100 GeV/c and its dependence on altitude studied between 0.6 and 36 km a.s.l. We discuss here some preliminary results and their importance. A positive muon analysis is in progress and the results will hopefully be available at the Conference.

1. INTRODUCTION

In the past, the muon flux has been studied in order to examine cosmic ray interactions in the atmosphere. The main source of muons in the momentum range investigated in this work is the decay of pions produced in hadronic interactions of cosmic rays. The contribution from kaon decay increases above a few hundred GeV/c. While sea-level measurements are widely reported in the literature, there are only a few measurements of the muon flux as a function of altitude (Conversi, 1950, Blokh *et al.*, 1977). This measurement can serve two purposes: a check for cosmic ray cascade calculations and for atmospheric neutrino calculations (Gaisser *et al.*,1988, Lipari, 1993). The main difficulty in performing a muon measurement at or above stratospheric altitudes is to properly compensate for the contamination of the muon sample by other particles. This problem becomes even more complex for positive muon measurements, since the proton flux strongly increases with altitude.

2. EXPERIMENTAL SETUP

The MASS apparatus consists of [1] a superconducting magnet spectrometer with 8 multiwire proportional chambers (MWPC), [2] a time of flight (TOF) system with 2 planes of 2 scintillator layers each, [3] a high resolution scintillator-the TOF system and the scintillator providing 5 independent dE/dx measurements-, [4] a gas Cherenkov detector and [5] a streamer tube imaging calorimeter. A coincidence between the TOF scintillators gives the trigger for data acquisition. Before transmitting the data to the ground an on-board computer checks that the pulse height in the high resolution scintillator is greater than 0.25 times that corresponding to a minimum ionizing particle. The Cherenkov detector is filled with a 50-50 mixture of Freon 12 and Freon 22 with a Lorentz threshold factor of 23. The calorimeter consists of 40 layers of 64 streamer tubes each and it is 7.3 radiation lengths and 0.7 nuclear interaction lengths long. More details on the apparatus characteristics and performance are given elsewhere (Golden *et al.*, 1991, Golden *et al.*, 1991b, De Pascale *et al.* ,1993).

3. DATA ANALYSIS

The dE/dx measurements from the scintillators and the hit pattern in the calorimeter were used to identify muons. The Cherenkov signal was used to estimate the fraction of contaminating electrons in the muon candidate sample. The TOF measurement was used to reject upward moving particles. Muons were required to have a signal between 0.5 and 2.0 I_0 in the high resolution scintillator and in the two uppermost scintillator layers of the TOF system, I_0 being the pulse height for a minimum ionizing singly charged particle. Muon candidates were also required not to have a shower in the calorimeter. The latter condition was imposed by considering the calorimeter divided into two parts and by selecting events with a number of hits n, $2 \leq n \leq 9$ for the upper part along the x- and y-views and $3 \leq n \leq 12$ for the lower part along the x-view (the lower part y-view was not operated during the flight). For a reliable determination of the particle curvature the muon events were also requested to satisfy MWPC data cuts as discussed in De Pascale *et al.*, 1993.

4. RESULTS AND DISCUSSION

The negative muon momentum spectrum has been measured at several altitudes, and the results are shown in Figure 1 through Figure 7. The exposure time as well as the altitude-dependent deadtime fraction were considered in evaluating the absolute fluxes. The tracking efficiency of the spectrometer and the geometric factor of the apparatus are energy dependent and are discussed in De Pascale *et al.*, 1991. The average values of the geometric factor and the spectrometer efficiency for negatively charged particles are reported in Table 1 for different momentum intervals. The calorimeter efficiency for muon tracks satisfying the above criteria was found to be 0.82 and a scintillator efficiency of 0.82 was assumed. An additional correction of 0.77 was considered in order to take into account the inefficiency due to the trigger system, the TOF measurement and the ground computer data transfer. At this point of the analysis, there could be an overall uncertainty of about 20% in the estimate of the total efficiency.

Momentum Interval (GeV/c)	0.3 0.46	0.46 0.63	0.63 0.89	0.89 1.18	1.18 1.58	1.58 2.22	2.22 3.55	3.55 8.	8. 100.
Geom. Factor (cm^2 sr)	81.5	107.4	117.2	122.4	125.0	126.5	127.5	128.0	128.1
Spectrometer Efficiency	0.52	0.58	0.63	0.67	0.69	0.69	0.69	0.69	0.69

TABLE 1: Momentum-dependent spectrometer efficiency and geometric factor of the apparatus for negative particles.

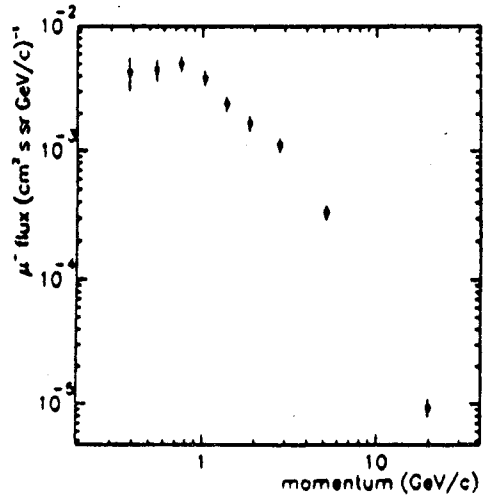

Fig. 1: Negative muon spectrum at 615 g/cm^2 average payload depth.

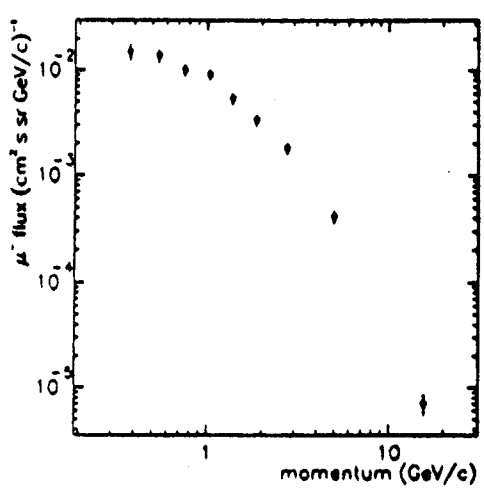

Fig. 2: Negative muon spectrum at 283 g/cm^2 average payload depth.

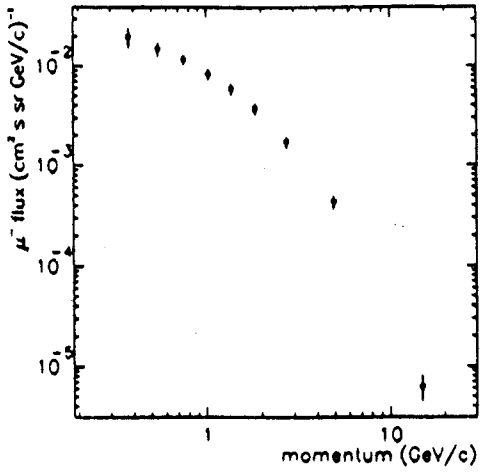

Fig. 3: Negative muon spectrum at 163 g/cm^2 average payload depth.

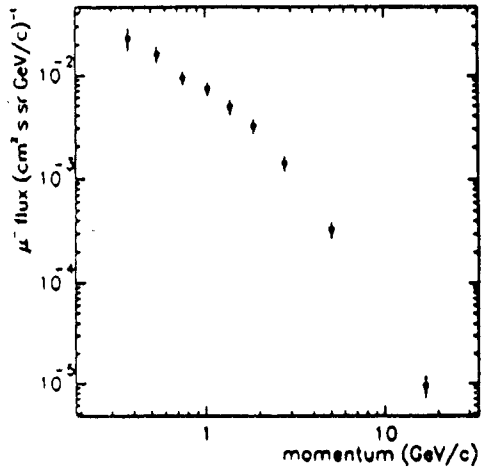

Fig. 4: Negative muon spectrum at 112 g/cm^2 average payload depth.

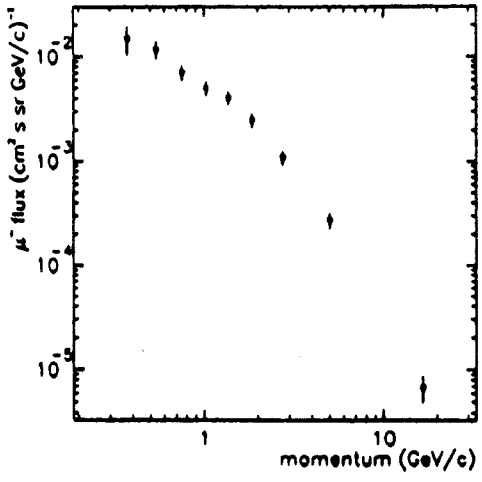

Fig. 5: Negative muon spectrum at 72 g/cm^2 average payload depth.

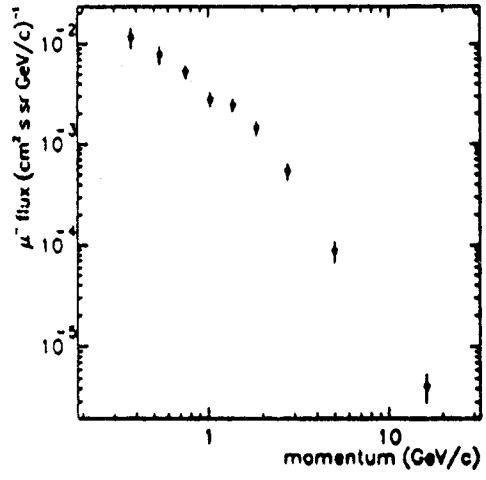

Fig. 6: Negative muon spectrum at 37 g/cm^2 average payload depth.

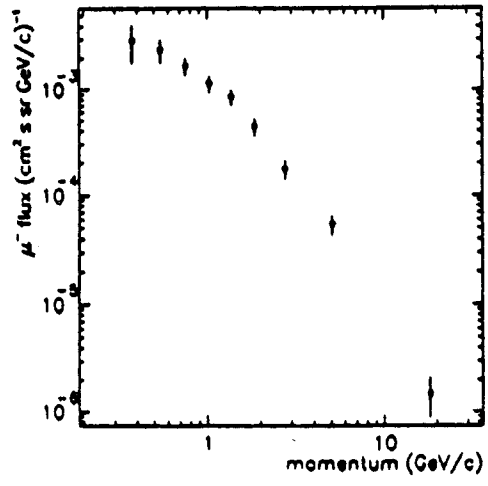

Fig. 7: Negative muon spectrum at 11 g/cm^2 average payload depth.

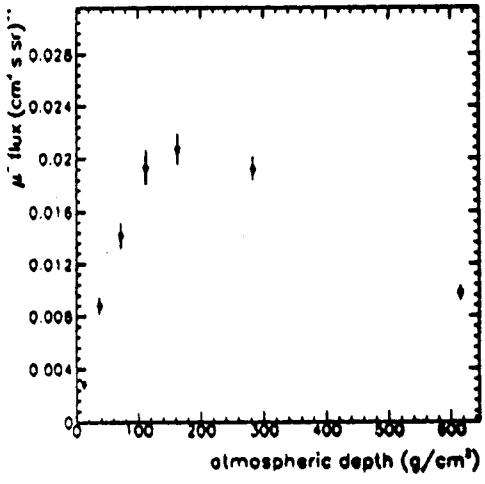

Fig. 8: Total negative muon flux in the 0.3-100 GeV/c momentum interval. Data are plotted at the average payload working depths.

At momenta less than 2 GeV/c, where the electron showers in the calorimeter become difficult to detect, the Cherenkov detector was used to get an estimate of the fraction of electrons in the muon sample and the flux values were corrected accordingly. The fraction of contaminating electrons at low energy is a function of energy and altitude. We are rather confident that no electron contamination should affect the measured flux at momenta above a few GeV/c. In order to account for the poorer resolution of the spectrometer at high energies, the number of spill-over particles, estimated by convolving the spectrum of the positive particles that survive the negative muon selection criteria with the resolution function of the spectrometer, was subtracted from muons in the highest energy bin. The possible contamination by pions and kaons was also studied, by comparing the present results with theoretical calculations at several altitudes in the atmosphere (Badhwar *et al.*, 1977). There could be an altitude-dependent pion contamination of the order of a few percent in the muon sample. The kaon contamination should be much smaller.

The negative muon flux has also been measured at the float altitude of 5 g/cm^2. The float altitude observations are reported in a separate paper at this Conference (Grimani *et al.*, 1993).

5. CONCLUSION

Data in Figure 8 can be used in order to evaluate the vertical profile of the negative muon flux in the atmosphere. This curve will serve both as a check on cosmic ray flux calculations in the atmosphere and as a boundary condition for atmospheric neutrino calculation. This is the first measurement of the muon flux as a function of altitude made over such a large altitude range with a single instrument. The room here is not enough to show all our results. They will be available at the Conference. The current evidence is that the flux profile is momentum dependent, the low energy muon flux peaking around 120 g/cm^2 and the higher energy muons penetrating to larger depths in the atmosphere. The spectral distribution of muons is affected accordingly.

ACKNOWLEDGMENTS

This work was supported by NASA grant NAG-110, the Istituto Nazionale di Fisica Nucleare, Italy and the Agenzia Spaziale Italiana. A very special thank to our technical support staff from NMSU and INFN.

REFERENCES

Badhwar G. D. F., *et al.*: 1977, Phys. Rev., D15, 820
De Pascale M. P., *et al*: 1993, J. G. Res., 98, 3501
Blokh YA. L., *et al.*: 1977, Nuovo Cimento, 37B, 198
Conversi M.: 1950, Phys. Rev., 79, 5
Gaisser T. K., *et al.*: 1988, Phys. Rev., D38, 85
Golden R. L., *et al.*: 1991, Nucl. Instr. Meth., A306, 366
Golden R. L., *et al.*: 1991b, PAL technical note # 224, available on request
Grimani C., *et al.*: 1993, presented at this Conference
Lipari P.: 1993, submitted to Astroparticle Phys.

Calgary 1993 XXIII ICRC HE 5.1.12 v.4

Negative Muon Spectrum at 5 g/cm^2

C. Grimani[6], S. A. Stephens[2,7], G.Basini[1], F. Bongiorno[1], F. Massimo Brancaccio[1], M. T. Brunetti[6], A. Codino[6], R. L. Golden[2], B. L. Kimbell[2], M. Menichelli[6], M. Miozza[6], A. Morselli[3], J.F.Ormes[4], P. Papini[5], M. P. De Pascale[3], P. Picozza[3], M. Ricci[1], I. Salvatori[6], P. Spillantini[5], S. J. Stochaj[2], R. E. Streitmatter[4], W. R.Webber[2]

1. INFN-Laboratori Nazionali di Frascati, Italy 2. New Mexico State University, New Mexico, USA 3. Dipartimento di Fisica and INFN dell'Universita' di Roma "Tor Vergata", Italy 4. NASA - Goddard Space Flight Center, Maryland. USA 5. Dipartimento di Fisica and INFN dell'Universita' di Firenze, Italy 6. Dipartimento di Fisica and INFN dell' Universita' di Perugia, Italy 7. Tata Institute of Fundamental Research, Bombay, India 8. Dipartimento di Fisica and INFN dell'Universita' di Roma, Italy.

ABSTRACT

The negative muon spectrum at 5 g/cm^2 (atmospheric depth)has been measured in the momentum range 300 MeV/c - 15 GeV/c with the MASS experiment. This experiment was flown on September 5th 1989. The flight was launched from Prince Albert , Canada and spent about 5.5 hours at float. We present our preliminary results and compare them to theoretical calculations.

1. INTRODUCTION

The study of the muon flux at different atmospheric depths, provides information about how primary cosmic rays interact with and propagated through the atmosphere. At 5 g/cm^2, a typical atmospheric depth for balloon-borne experiments, muons in the energy range of the experiment are mainly generated by the decay of pions which are produced in hadronic interactions of primary cosmic rays with the atmosphere above the instrument. Kaon decay becomes an important source of muons above 100 GeV. Theoretical calculations have been carried out by several authors (Badhwar et al. (1977), Stephens (1981)). Negative muon measurements at balloon altitudes are made difficult by poor statistics and electron background. To our knowledge, this is the first negative muon measurement ever carried-out at 5 g/cm^2. We believe that this measurement is of great interest since these muons can give rise to neutrinos which can act as background for underground neutrino experiments.

2. EXPERIMENT

The MASS apparatus consisted of a magnetic spectrometer, a scintillator TOF system, a high resolution scintillator, a gas-Cherenkov detector and a streamer-tube calorimeter. The magnetic spectrometer and its performance, are described in Golden et al. (1991). A coincidence between the scintillator paddles of the TOF system generated the trigger for the experiment. The high resolution scintillator was located directly above the spectrometer and served as an entrance plane for the tracking system. In order to limit the number of events that miss the active volume of the tracking system, the on-board computer checked that the pulse-height in the high resolution scintillator is greater than 0.25 times the signal for a minimum ionizing particle before transmitting the events to the ground. The Cherenkov detector was filled with a 50 - 50 mixture of Freon 12 and Freon 22. This corresponds to a threshold Lorentz factor of 23. The Cherenkov counter consisted of a segmented mirror which focused the Cherenkov light on four phototubes. The calorimeter was comprised of 40 layers of brass streamer tubes. Each layer was divided into 64 cells. The 40 layers represent a total of 7.3 radiation lengths and 0.7 nuclear interaction lengths. The calorimeter data allows the topological structure of the particle's interaction to be reconstructed. (More details of the apparatus performance and characteristics are given in Basini et al., 1991 and references therein).

3. DATA ANALYSIS

In order to obtain the negative muon flux, the muon events must be separated from all other negative curvature events. Electron, antiprotons and upward moving albedo protons comprise the majority of the background events. The data analysis has been carried out using different criteria below and above the Cherenkov threshold for muons (2.4 GeV).

In the momentum range up to 2 GeV/c, where electrons are above the Cherenkov threshold, muon candidates were selected as particles that did not generate a Cherenkov signal (Cherenkov pulse-height <1 photo-electron). The chance rate for accidental Cherenkov signals has been found to be $5x10^{-4}$. The low energy albedo protons were removed by using the TOF measurement. With a resolution of 256 ps, upward moving particle are separated form downward moving particles by more that 25 sigma.

Above 2.5 GeV/c muon candidates were selected as singly charge ionizing particles showing a Cherenkov signal. This cut removed the possible antiproton contamination since the antiproton Cherenkov threshold corresponds to 21.4 GeV. In order to remove electrons from the events above 2.5 GV/c, we required the muon candidates to have a single straight track in the calorimeter (i.e. no more than 2 calorimeter planes can show a shower cluster, Basini et al., 1991). This constraint was not applied at lower energies because the low energy electrons do not reliably show a clear shower in the calorimeter. Near the muon Cherenkov threshold (in the momentum range 2.0 - 2.5 GeV/c), the Cherenkov counter has a high inefficiency for muon detection. In this same range, the calorimeter also does not provide good discrimination of electrons and muons. Thus we do not report muon fluxes in the 2.0 - 2.5 GeV/c.

4. RESULTS

The muon flux obtained with our measurement is shown in Fig. 1 along with theoretical calculations (Stephens, 1981). In order to estimate the absolute flux, corrections were made for the geometric factor, the exposure time and the selection efficiencies. In the energy range up to 2 GeV the geometrical factor and the chamber efficiency are energy-dependent. This dependence has been discussed in De Pascale et. al., 1993. In this energy range the total elapsed time was of 12600 s. The dead-time associated with on board data processing was measured with an on-board timer. It was found to be 33% of the total elapsed time. Efficiencies for the Z=1 selection in the TOF system was found to be 0.97. The correction to the trigger geometry was found to be 0.82. Finally the live-time efficiency of the taper recording process was found to be 0.94. Above 2 GeV, we included data for the total elapsed time (19812 s) estimating the loss of particles for the events hitting the mirror while the phototube was not working. This loss of particles results in an additional Cherenkov inefficiency. Total efficiencies and data for flux calculation are given in Table 1. Also, in the energy range above 2.0 GeV/c, we used a restricted geometry, in order to assure that electron showers were completely contained in the calorimeter (Basini et al., 1991). This restricted geometrical factor is constant and equal to 80 cm^2 sr, and the trigger geometry correction was 0.90. Electron contamination in the low energy sample, due to the Cherenkov inefficiency for electrons (efficiency is 0.98) has been estimated considering the electron flux at the time of the flight (Basini et al. 1991). Below 1 GeV the contamination is about 1% and between 1 and 2 GeV about 3%. The possible contamination of negative pions and kaons in the muon sample has been studied (Stephens, 1981). The kaon flux at 5 g/cm^2 is of several order of magnitude smaller than the muon flux. We estimated a pion contamination at energies greater than 3 GeV to be a few percent and less than 1% at smaller energies.

Table 1

Kin. En. Interval (GeV)	Number of Events	Geom. Factor (cm^2 sr)	Total Efficiency	Flux (part/(m^2 sr s GeV))
0.213-0.318	94	74.6	0.257	40.96±4.22
0.308-0.406	119	94.0	0.282	36.36±3.33
0.406-0.504	126	104.6	0.299	32.63±2.90
0.504-0.603	95	113.3	0.316	21.27±2.18
0.603-0.702	83	117.0	0.325	17.50±1.92
0.702-0.801	77	119.2	0.332	15.60±1.78
0.801-0.900	61	120.8	0.338	11.98±1.53
0.900-1.10	98	121.9	0.338	9.44±0.95
1.10-1.30	84	123.7	0.342	7.88±0.86
1.30-1.50	64	125.0	0.343	5.92±0.74
1.50-1.90	73	126.2	0.343	3.35±0.39
2.42-3.91	62	80.0	0.148	1.77±0.22
3.91-5.90	36	80.0	0.284	0.40±0.07
5.90-8.90	22	80.0	0.306	0.15±0.03
8.90-14.90	8	80.0	0.306	0.027±0.01

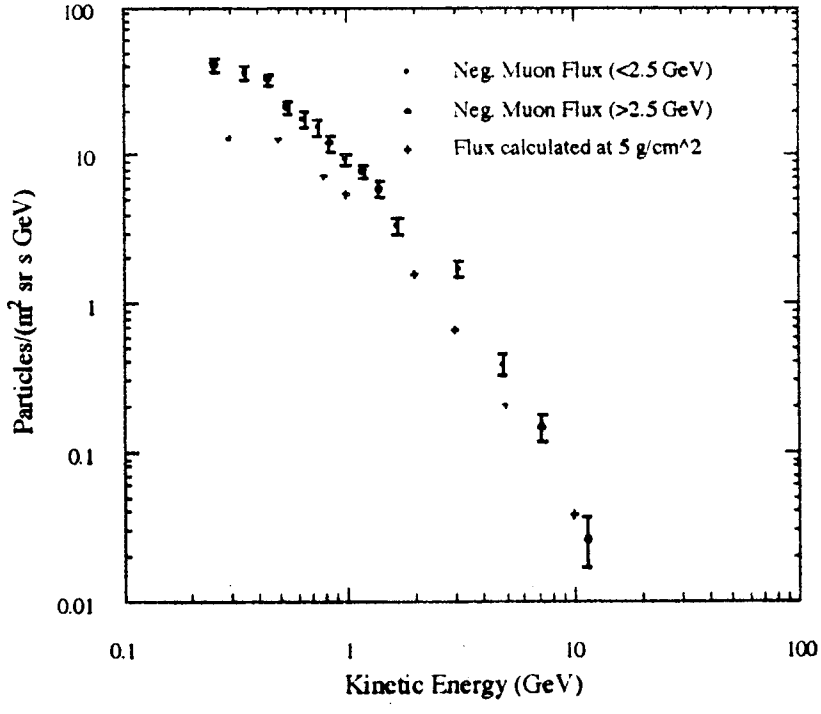

Fig 1 : Measured and calculated negative muon flux as a function of kinetic energy

5. DISCUSSION

Figure 1 shows that at lower energies (0.4 - 1.0 GeV), the observed muon flux is about two times greater than predicted. At 3 GeV the fluxes again differ by about a factor of 2 but above that energy the observed spectrum falls more rapidly than predicted. We are currently investigating the possibilities of errors in event selection, efficiency determination and in the prediction to try to resolve the differences. The reader is reminded that the muons are difficult to identify and that absolute fluxes require painstaking care in the efficiency measurements.

Muon fluxes lower in the atmosphere are reported in a separate paper at the conference (Circella et al.,1993)

6. ACKNOWLEDGMENTS
This work was supported by NASA grant NAG-110, the Istituto Nazionale di Fisica Nucleare, Italy and the Agenzia Spaziale Italiana. A very special thank to our technical support staff from NMSU and INFN.

REFERENCES

Badhwar G. D., Stephens S. A., Golden R. L.:1973, Phys. Rev., **D 1 5**, 820.
Basini G.et al.:1991, Proc., 22th Internat. Cosmic Ray Conf., Dublin (Ireland),**2**, 137, also submitted to Ap. J.
Circella, M., et al.:1993 presented at this conference
De Pascale, et al.:1993, Journal of Geophysical Research, **9 8** 3501.
Golden R. L. et al.:1991, Nucl. Instr. Meth., **A 3 0 6**, 366.
Golden R. L. et al.:1979, Phys. Rev. Lett. ., **4 3**, 1264.
Stephens S. A.: 1981, Proc. 17th Internat. Cosmic Ray Conf., Paris (France),**4**, 282. .

Calgary 1993 XXIII ICRC SH 8.1.6 v.3

Ground Level Observation Of Electrons, Positrons and Protons

G. Basini[3], F. Bongiorno[3], M.T. Brunetti[6], A. Codino[6], R.L. Golden[1], C. Grimani[1,6], B.L. Kimbell[1], F.Massimo Brancaccio[3], M. Menichelli[6], M. Miozza[6], A. Morselli[2], J.F. Ormes[4], P. Papini[5], M.P. De Pascale[2], P. Picozza[2], M. Ricci[3], I. Salvatori[6], E.S. Seo[4], P. Spillantini[5], S.A. Stephens[1,7], S. Stochaj[1], R.E. Streitmatter[4] and W.R. Webber[1]

1. New Mexico State University, Las Cruces, NM 88003, USA; 2. Dipartimento di Fisica and INFN dell' Universita' di Roma "Tor Vergata",Italy; 3. INFN-Laboratori Nazionali di Frascati, Frascati,Italy; 4. NASA-Goddard Space Flight Center, Greenbelt, Maryland, USA; 5. Dipartimento di Fisica and INFN dell' Universita' di Firenze,Italy; 6. Dipartimento di Fisica and INFN dell' Universita' di Perugia, Italy; 7. Tata Institute of Fundamental Research, Bombay, India.

ABSTRACT

Analysis of the energy spectra of electrons and protons was carried out using ground data recorded in Prince Albert, Canada by the MASS experiment. We present the preliminary results on the energy spectra at an atmospheric depth of 945 g/cm^2 in the momentum interval 0.125 to 2.5 GeV/c for electrons and 3.7 to 20.0 GeV/c for protons.

1. INTRODUCTION

The observed cosmic ray spectra at ground level result from the propagation of primary cosmic rays in the atmosphere. This radiation consists mainly of weakly interacting muons. Most of the protons at ground level are the surviving fraction of the primary nucleons after ~ 11 interaction mean free paths; the electrons result from cascade processes in the atmosphere. An accurate determination of the spectra of these components gives information on the physical processes involved in the propagation and on the composition of the primary component. It also provides a standard source for the calibration of detector systems. Only a few attempts have been made in the past to measure their spectra at sea level. In the experiment described here, we used a superconducting magnet spectrometer, which was also deployed to study the primary and secondary cosmic rays at the top of the atmosphere (Basini et al, 1991 & 1993; Grimani et al, 1993) and muon component during the ascend of the balloon (Circella et al, 1993). We compare our observed spectra on proton and electron components with other experimental results and with theoretical calculations.

2. EXPERIMENT

The MASS apparatus consisted of a magnet spectrometer with multiwire proportional chambers (MWPC), scintillators, a gas Cherenkov detector and a calorimeter, to measure respectively, the rigidity and sign of charge, charge and time of flight, velocity and shower profile. This magnetic spectrometer was

described by Golden et al (1991) and the trigger criteria for recording events were given in De Pascale et al(1993). To briefly describe the detectors, the Cherenkov detector consisted of a segmented mirror to focus the Cherenkov light on four phototubes and was filled with a mixture of Freon 12 and Freon 22, having a threshold Lorentz factor of 23. The time flight device had 2 planes, each with 2 layers of scintillators separated by 2.4 m; an additional high resolution scintillator was used for charge measurement. The calorimeter consisted of 40 layers each with 64 brass streamer tubes; the alternate layers of tubes being perpendicular to each other. It had an effective depth of 0.75 interaction length for protons. This experiment was carried out in Prince Albert, which was located at 53N & 106E, and 600m above sea level. The data were recorded on August 30, 1989 for a period of about 17 hours. In the present analysis, we have restricted the energy interval for electrons from 0.125 to 2.5 GeV, and protons from 2.76 to 19.06 GeV.

3. SELECTION OF EVENTS

The selection criteria used for an event to have a good trajectory in the spectrometer were the same as those described in De Pascale et al (1993). The criteria used for selecting electron-positron events were similar to those in Basini et al (1991). After selecting singly ionizing particles, we applied signals from the Cherenkov detector and calorimeter for further analysis. Below 500 MeV, where the number of electromagnetic shower particle is small, we selected events accompanied by a Cherenkov signal corresponding to > 1 photoelectron; the accidental rate for such signal was only 5×10^{-4}. Between 500 MeV and 2.5 GeV we included additional calorimeter constraints as we were approaching the Cherenkov threshold for muons(2.4 GeV). We required that an event to show > 6 cells to be activated in the first nine planes of the calorimeter and that single cell activation should not be in more than 9 planes in a region of 5 cells around the particle trajectory projected from MWPCs. A total of 282 e^- and 199 e^+ were identified.

In the case of protons we selected singly ionizing events with positive curvature and with no Cherenkov signal. We also required that the calorimeter has multiple tracks in order to select proton interaction in the calorimeter. These events were examined visually for interaction vertex to confirm that the event is due to a proton. Proton selection was made in the restricted geometry as in the case of electrons (Basini et al, 1991). A total of 69 protons were identified. This number was corrected for non-interacting ones in the calorimeter. To look for any selection bias resulting from backward going secondary particles in to the MWPC, we divided the calorimeter into two sectors. We had 41 interactions in the upper half and on this basis we expected 28 in the in the lower half and we found 30 $\pm$ 5.5 which is in good agreement with the expectation.

4. RESULTS

The electron spectrum is shown in the lower part of Fig.

1. In computing the flux, the geometric factor was estimated to be 85.4 $cm^2.sr$ which decreases below 1 GV. The spectrometer efficiency for selecting good tracks was 0.69, which also decreases below 4GV, and we have taken care of selection efficiencies relating to Cherenkov, scintillator, tape reading and trigger (see De Pascale et al, 1993; Basini et al,1991).It appears that the spectrum below 0.3 GeV is steeper than it is above this energy. We are examining at this stage any bias due to the sharp decrease in the estimated geometric factor in these energy regions. For comparison, we have shown the measurements by Beuermann & Wibberenz (1 968)corrected for the present altitude by the electron attenuation mean free path given by Daniel & Stephens (1974). We have also shown by solid curve, the theoretival estimate by Daniel & Stephens which falls in between the two experimental results. The e^+/e^- ratio is shown as a function of energy in the same figure and one can notice an excellent agreement with the theoretical expectation.

The estimated proton flux values are plotted in Figure 2. This spectrum can be represented by a powerlaw in momentum with a spectral slope of -3.0 $\pm$.3 and in kinetic energy as

$$J(E) = 5.5\ E^{-2.7\ \pm 0.25}$$

proton / (m^2.sr.s.GeV). This spectral slope is in good agreement with that of the primary spectrum. For a comparison we have shown the measured flux values at sea

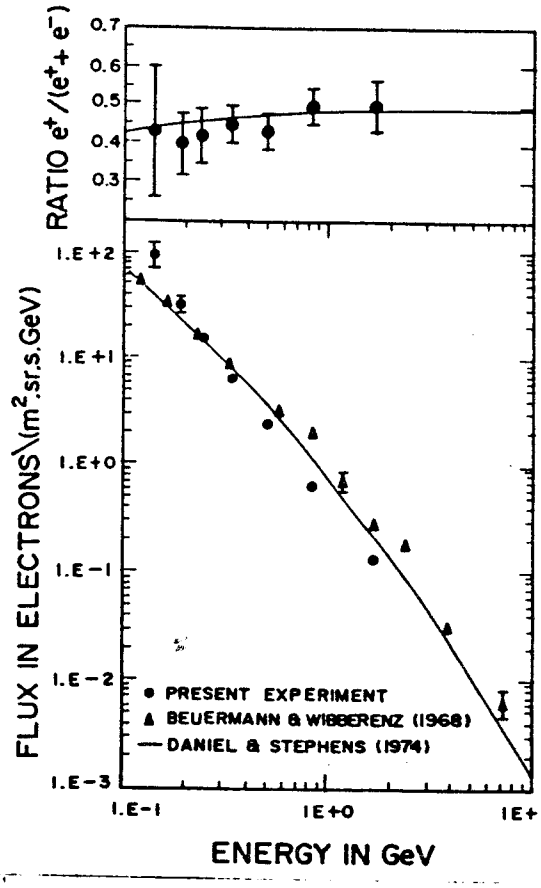

Fig.1 The energy spectra of $e^+ + e^-$ are shown in the lower part and the charge ratio in the upper part.

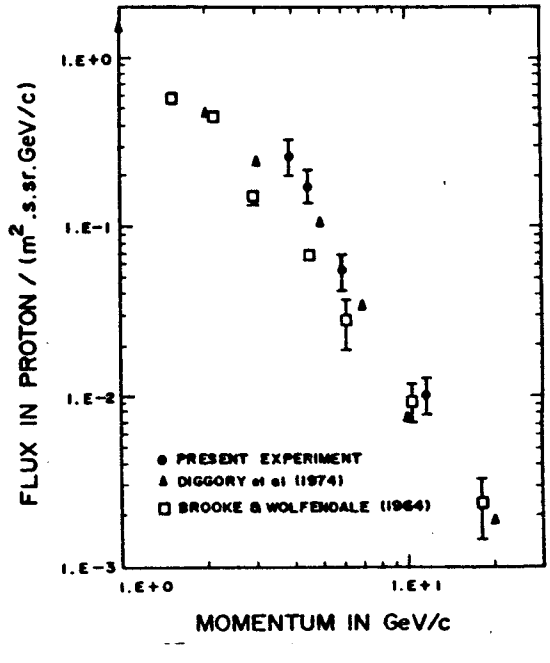

Fig.2 Proton spectrum is shown as afunction of momentum.

level (Diggory et al, 1974; Brooke & Wolfendale, 1964) multiplied by exp (85/120) to elevate to the present depth of 945 g/cm**2. One can notice that our flux values are higher than the earlier measurements.It may be pointed out that in the earlier measurements, the flux values were obtained by normalizing the integral muon flux measured in the same experiment to some standard values, while we determined the absolute flux values. The ratios of protons to muons are plotted in Figure 3. It can be seen here that there is a noticeable difference between our results and those of Brooke & Wolfendale. Since our spectral slope is in agreement with the primary spectrum and that the measured muon spectral shape flattens below about 30 GeV/c, we believe that our proton measurements are reliable. It may be pointed out that the muon spectrum obtained by us is in excellent agreement with other measurements and with theoretical expectations (De Pascale et al, 1993). Therefore, we conclude that either the proton flux or the muon spectrum below 20 GeV/c, measured by Brooke & Wolfendale could be in error. It will be interesting to extend the proton spectrum to lower energies to look for the effect of ionization, which flattens the spectrum below 2 GeV/c. We also show the electron to muon ratio as a function of momentum in Figure 3 in the region from 0.3 to 2.5 GeV/c and it can be seen that the soft component at ground level contributes more than 10% of the radiation below 200 MeV/c, but decreases to < 1% above 1 GeV/c.

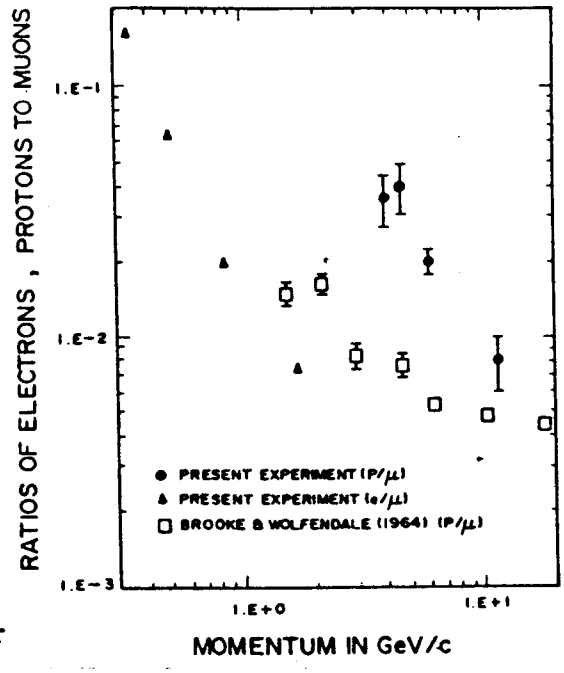

Fig.3 The ratios of electrons & prons to muons are plotted as a function of momentum.

REFERENCES

Basini,G et al:1991,Proc.22nd Int.Cosmic Ray Conf.(Dublin), 2,137; under publication in Ap. J.
Basini,G et al:1993 at this Conference
Beuermann,KP and Wibberenz,G:1968,Can.J.Phys.,46,S1034
Brooke,G and Wolfendale,AW:1964,Proc.Phys.Soc.London,83,843
Circella M et al:1993, at this Conference
Daniel,RR and Stephens,SA:1974,Rev.Geophys & Sp.Phys.,12,233
Diggory,IS et al:1974,J.Phys.,A7,741
Grimani,C et al:1993, at this Conference
Golden,RL et al:1991,Nucl.Instr.Meth.,A306,366
De Pascale, MP et al: 1993 J.Geophys.Res.,98(A),3501

Calgary 1993 XXIII ICRC OG 10.5.18 v.2

A transition radiation detector for positron identification in particle astrophysics experiments

R.Bellotti, F.Cafagna, M.Calicchio, M.Circella,G.De Cataldo, C.De Marzo, O.Erriquez, C.Favuzzi, P.Fusco, N.Giglietto, B.Marangelli, A.Rainò, and P.Spinelli
Dipartimento di Fisica dell'Università di Bari and INFN Sezione di Bari, Italy

Abstract

We have built and tested a transition radiation detector (TRD) to discriminate positrons from protons in an experiment to be performed on ballon flights to search for primordial antimatter .We achieve a proton -electron rejection factor of the order of 10^{-3} with a power consumption of about 40 mW per MWPC channel .

1. Introduction

We have prepared a TRD for a cosmic ray space experiment to be performed on the NASA balloon-borne magnet facility (BBMF) in this year [1]. The item we intend to investigate is whether the e^+/e^- ratio really increases above 15 GeV and, in addition, whether the e^+/p ratio indicates any signs of energy losses for positron.For positron identification from 4 to 50 GeV (limit imposed by the exposure time) we intend to use a TRD. Since the e^+/p ratio is expected in the range from 10^{-3} to 10^{-4} , we need to rely on a detector which has the probability to identify erroneously a proton as a positron of the order of 10^{-5} or less. For this purpose we will employ an imaging calorimeter in conjunction to the TRD; taking into account the performance of the calorimeter we require for the TRD a rejection factor against protons of the order of 10^{-3} .

2. TRD description

The TRD is based on ten modules each consisting of a carbon fiber radiator followed by a multiwire proportional chamber.Each radiator consists of an aluminum frame containing four polyethylene bags filled with carbon fiber segments 6 mm long, 7 μm thick , and has overall dimensions of 80x80x5 cm^3. Its density has been fixed to the optimal value of 0.060 g/cm^3 . The proportional chambers have an active surface of 78x80 cm^2 and consist of four square frames of Stesalit material . The first and fourth frames are equipped with 23 μm thick Mylar foils internally graphite painted to 50 KΩ/square to work as cathode planes. The anode plane contains 256 gold plated tungsten wires, 25 μm thick, 3 mm spaced apart.We have used no additional windows in this chamber design.In order to withstand cathode planes deformations due to pressure unbalance between chamber inner and outer gases the Mylar foils have been reinforced by a grid of fiber glass strips stretched ,on the thiner edge,across the Stesalit frames. The chambers are operated with a

xenon (80%) - methane (20%) mixture chosen to give optimal TR photon conversion with low δ-ray background production. The ten modules are stacked in a light aluminum rack enclosed inside an aluminum box.This box ,designed to withstand a 10 G shock, is sealed by a flange which allows only the terminal part of the MWPCs printed boards to come out to allow them to be connected to the read-out electronics (Fig 1) . The balance between the chamber gas inner pressure and the outer box pressure is obtained by permanently flowing into the two volumes the xenon -methane mixture and methane respectively at fixed rate. The two flows are regulated by two valves remote controlled by a unit MKS 1250A and two pressure sensors.The differential pressure tolerated between the chamber and the box volume,and between the box and the gas inside the balloon payload is 50 μbar .

3. TRD electronics description

Chambers signal processing is based on the "cluster counting" technique [2] which ensures that the rejection factor results quite stable with respect to signal amplitude variations . In order to reduce the power consumption to about 40 mW/channel to limit the overall power to about 100 Watt ,as allowed for the TRD during the flight ,we have developed in collaboration with LABEN company a new front end electronic channel based on hybrid circuitry technology. The channel layout is shown in fig. 2. The first block delimited by the dotted box corresponds to a hybrid circuit containing the preamplifier while the second one corresponds to the amplifier and the discriminator chain. The discriminator output is delayed by 110 nsec and sent to an AND-gate in time with the external trigger gate G. This trigger signal is formed by coincidence pulses of the beam defining counters and has a width of 350 nsec to account for the drift time of clusters towards the anode wire. The pulses passing the AND-gate are counted by a 4 bit counter and transferred to a CAMAC interface module to be read out into the on line computer. All the components used immediately downstream the discriminator are based on HCMOS family to get both low power consumption and fast switching in order to correctly count the cluster pulses. With this layout the overall measured double pulse resolution is 25 sec.

The read -out electronics consists of two main blocks: the first one examines the wire counters and writes their contents, if any,in a buffer memory; the second one is a CAMAC interface module which handles the data transfer from the buffer memory to the computer of the experiment .Fig 3 shows the block schematics of the first part of the read-out electronics ,for a single MWPC.The principle of operation is briefly described .After an event has been accepted ,the number of clusters occurred on each wire is stored in the relative counter .The trailing edge of the GATE PULSE

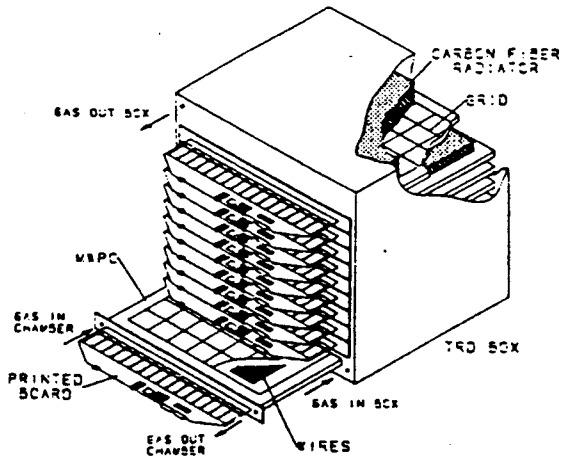

Fig. 1 - TRD artist's view

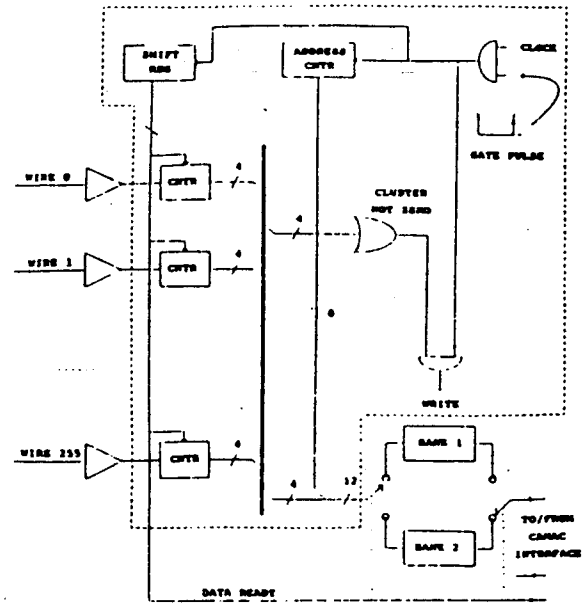

Fig. 3 - Read-out electronics schematics

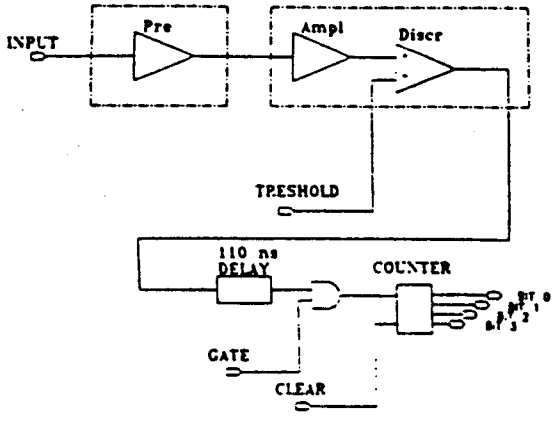

Fig. 2 - Electronic channel layout

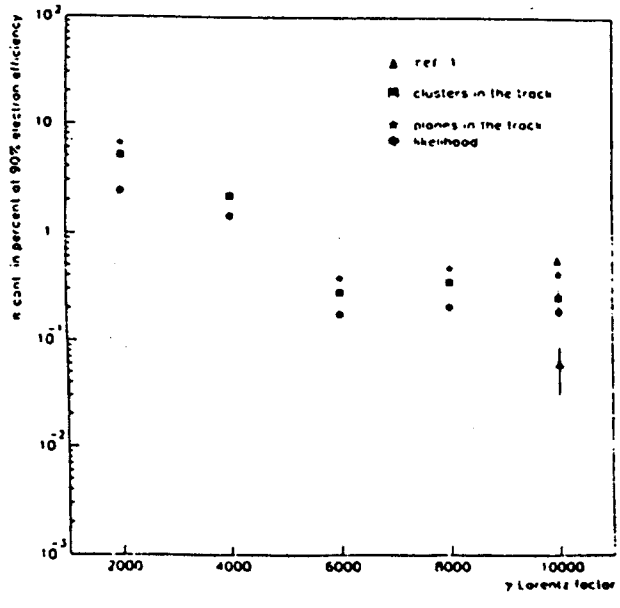

Fig. 4 - Pion contamination (in percent) versus electron efficiency. Stars: plane fired counting method. Squares: hit counting method. Dots: likelihood method. Open triangle: old electronics (ref. 3). Full triangle: ref.1

enables the 2.4 MHz clock,so the scanning of wire counters starts and,if the counter is not empty (CLUSTER NOT ZERO) ,the data are written in a buffer memory.The ten plane of the detector are scanned in parallel .With the use of a data bus , in place of the traditional daisy chain ,in case of failure of an element of the chain ,all the wires 'behind' that cell are not definitely lost. In order to improve data handling at high rates,two banks are provided.Blocks enclosed in dashed lines in Fig .3 were realized on Field -Programmable Gate Array (FPGA) . The dedicated CAMAC interface module not shown in the figure ,starts reading at the arrival of DATA ready from any of the ten planes of the detector .Data transfer from the planes is carried out sequentially

4.Tests and results

We have used the same pion/electron beam as shown in [3] to test the TRD equipped with this electronics. The beam momentum was varied from 1 to 5 GeV/c in steps of 1 GeV. In order to design and then test the performances of the TRD ,we first used a reduced scale prototype as described in [3] and [4] . Only a sample of the full size chambers and radiators were individually tested in the beam : no difference was observed in transition radiation photon yield, with respect to the reduced size prototype.The remaining chambers and radiators were calibrated with respect to the former ones by Fe 55 and Cd 109 X-ray sources .We have used the same likelihood procedure introduced by Cherry [5] to distinguish different mass particles by the relative cluster count distributions. With this procedure we achieve a pion rejection factor of about 2×10^{-3} beyond $\gamma = 6000$, as we can see in fig (4) where the result obtained at $\gamma = 10^4$,using the faster electronics used in [4] , is also reported. The result from a similar ten modules TRD [2] is also shown for comparison.We then tested the complete TRD by cosmic rays using a fine grained scintillator telescope to define a charged track crossing the detector and to generate the gate to the MWPCs.We got from the ten chambers a poissonian δ- ray distribution of same average ($n_\delta = 2.2$) as the ones measured with the prototype in the pion beam .

REFERENCES

[1] R.L.Golden et al., "Continuation of cosmic ray studies using balloon-borne superconducting magnet", Proposal submit. in response to NRA-90-OSSA-11, 1990.

[2] C. W. Fabjan et al., Nucl. Instr. and Meth. 181 (1981) 119.

[3] E. Barbarito et al., Nucl. Instr. and Meth.A313(1992) 295-302

[4] R.Bellotti et al.,Nucl. Instr. and Meth.A323(1992) 71-77

[5] M.L.Cherry et al.,Nucl.Instr.and Meth.115(1974) 141.

Calgary 1993 XXIII ICRC OG 10.3.8 v.2

WIDGET: A Data Acquisition System For A Balloon Borne Si Particle Calorimeter

Alberto Colavita[1,2], Piergiorgio Picozza[3],Fabio Fratnik[3],Pedro Battaiotto[4], Fernando Aversa[1], Srinivasan Venkataraman[1].

[1]Microprocessor Laboratory, ICTP/INFN, Via Beirut 31, 34100 Trieste, Italy
[2]On leave of absence: Universidad Nacional de San Luis, 5700 San Luis, Argentina.
[3] Italian National Institute of Nuclear Research, Tor Vergata, Italy.
[4] Universidad Nacional de La Plata, Argentina.

ABSTRACT

We describe Widget; a complete data acquisition system (DAS) designed for a balloon-borne calorimeter using silicon strip detectors. The design includes a general purpose CPU as well as five to twenty Digital Signal Processors in order to control the acquisition of the data. This local intelligence also allows the instrument to re-calibrate itself, to perform calculations on the data and to control the functionality of the instrumentation. The DSPs filter the data to avoid overflowing the radio link to ground. In principle the system could control the instruments, without direct intervention from the ground, on flights with durations of several days .

1. INTRODUCTION

Widget (Wizard Data Getter) is the data acquisition system for the balloon phase of the Wizard collaboration [1]. The ultimate purpose of the collaboration is to launch a satellite borne instrument capable of extending our knowledge in cosmic ray physics and related disciplines. This includes the search for primordial antimatter, the determination of the energy spectra of antiprotons and positrons up to a few hundred Gev and the measurement of energy and spectra of protons, electrons and nuclei up to Carbon.

The Wizard payload includes, in its various possible configurations, several other instruments besides the silicon calorimeter. The main concern of this paper is the data acquisition system of the silicon calorimeter.

The calorimeter provides discrimination of electrons from protons by measuring the energy deposited by the particles while passing through plates of tungsten. Electrons produce bremstrahlung photons, which in turn produce electron positron pairs, hence generating a particle shower. The slabs of high-Z material are alternated with planes of detectors to sample the development of the shower. The ability of the calorimeter to discriminate between electrons and proton resides in recognizing the different spatial development of both types of showers and in its energy resolution.

The collaboration chose silicon strip detectors as the detecting medium[2]. Silicon detectors are widely used in High Energy Physics (HEP) experiments. But, unlike its ground counterpart, air borne and space applications present additional requirements for the data acquisition system such as: low weight, low power consumption and high reliability.

Widget will be used for the already programmed balloon flights; two during 1993 and the remaining flight during 1994. Widget was designed and built using off-the-shelf components. The prototype system was designed to check the concept of massive computing power for balloon flights as well as to obtain relevant physics results.

For the satellite phase much of the electronics will be monolithic although the architecture will be the same. In particular, we will publish separately the details of the

monolithic implementation of the front end electronics, there are already prototypes in silicon and gallium arsenide, since it is an issue all by itself.

2. GENERAL ARCHITECTURE

In an accelerator environment, the usual role of a data acquisition system is to wait for a trigger signal to enter into action. Some fast electronics generates the trigger signal every time that it recognizes, in one event, some predetermined sought after characteristic. At that moment the data acquisition system reads all the signal channels, it converts the analog values into digital form, it builds the event and stores the data into some magnetic media in order to analyze it off-line. If the operator want to recalibrate the system or check its functionality the data taking is stopped and it resumes only after the procedure has been carried out. If a system failure is detected there is ample time and easy access to the electronics.

A balloon borne data acquisition instead has to perform all the aforementioned tasks and more. Since a typical flight lasts for some 25 hours, time is at a premium and no physical access to the electronics is available. Some of these extra tasks are: to control the functionality of the whole instrument, to filter and compress the data since it has to be downloaded to ground through a narrow bandwidth radio link, to recalibrate the systems because of temperature variations or aging, to locally store tha acquired data because the link is too slow or because the downloading is possible only at determined periods.

The fine details of the electronics and of the on-board software can be found in the technical literature written for the users of Widget [3][4].

Figure 1 shows the architecture of Widget. The main system architecture looks very much like a funnel, to have at all times and places, a data bandwidth and computing power coherent with the amount of data to be handled.

The first version of the calorimeter will fly with only five silicon detector planes, the second with seven and the last with thirteen planes. Hence, we designed a modular hardware architecture admitting up to 32 detector planes and capable of servicing 50-100 events per second regardless of the number of planes. This flexible data acquisition system required the following boards:a) the GMX a general purpose single board CPU[5] capable of running OS-9, a Real-Time operating system;b) the PiggyBoard ,a module provider of general services;c) the RomeModule, a board capable of generating test signals for the maintenance and in-flight calibration of the system;d) the FlashDisk, an ultra low power consumption solid state disk using a bank of FlashCards; e) the VoodooCards- one for each plane- they embody a digital signal processor (DSP), 16 A/D converters and a 4 kword double port memory (DPM). For the main processor we used a commercial single board computer while all the other boards were custom designed. We will refrain from describing here the FlashDisk since it is only needed when flying with more than five planes.

Figure 2 shows the data path for the signal coming from one of the Si strips. In what follows we will outline the acquisition of the data after the S/H circuit.

We assigned to each Voodoo one TMS320E25[6] DSP, running at 40 Mhz, to service all the functions of a plane. Each DSP acts sometimes as a CPU and at other times as a sequence[7], controlling the activity of the A/Ds and selecting those channel values that are above the electronic noise.

The analog signals are converted in parallel in all 16 A/D of a plane and in each plane. This high degree of parallelism provides a large throughput. Each highly integrated LM14458 A/D converter is capable of outputting a 12-bit+sign number at a rate of 87 ksamples/s. Also, the LM14458 can recalibrate itself, it goes into an standby mode if requested, it has 8 S/H inputs and a multiplexer that selects the channel to be converted and an internal 32 conversion deep FIFO. This IC is one of the first available data acquisition systems in a chip.

The DSPs filter the large amount of data generated for each event. Each plane has 256 data channels, and since the signal from each is passed through a x1 or x16 amplifier, the DSP has to compare 512 numbers against 512 different thresholds. The DSP writes into the DPM only the converted signals with values that are above the thresholds. The GMX reads out these values from the other side of the DPM, labeling and writing them, together with the data coming from the other planes, into the CamacCard. The onboard MicroVax reads the data from the Camac and it transmits these relevant data to ground through the radio link.

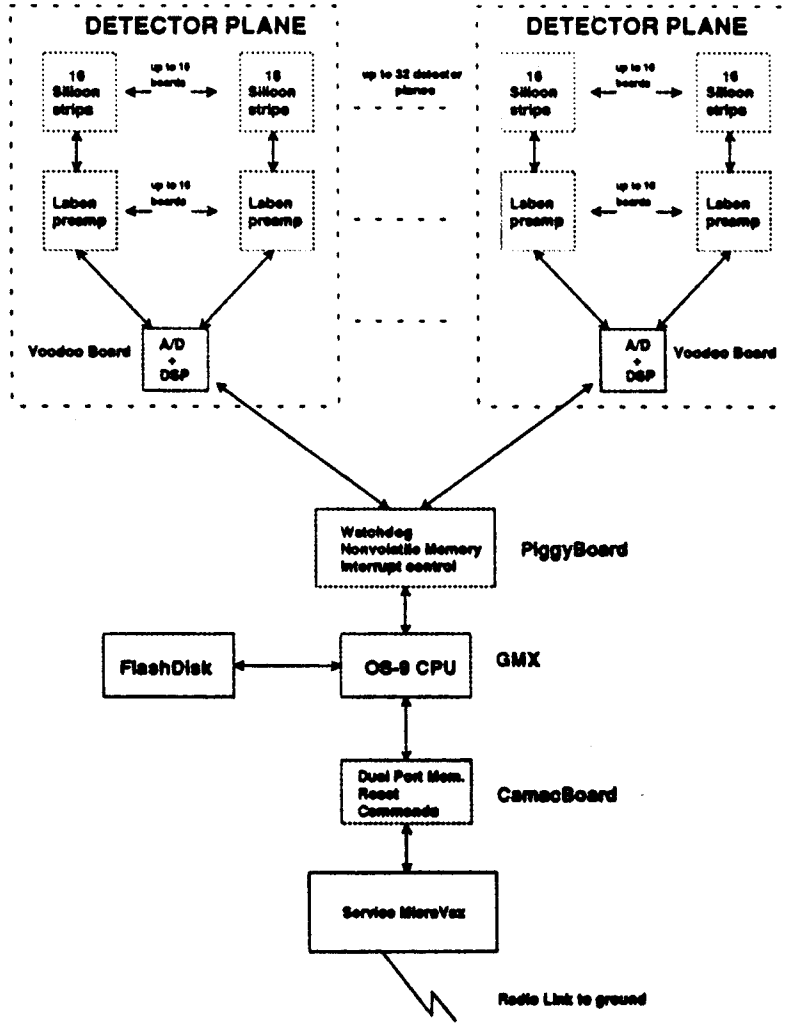

Fig. 1: General Architecture of the Si Calorimeter Data Acquisition System.

The GMX is the master of the system. After Reset it delivers to the DSPs the initial values for the thresholds, S/H times, and programs for the A/D. These programs instruct the A/D to acquire the data from any of the 8 channels of the multiplexer, either versus ground or differentially. A reference voltage is connected to one of the input channels. This voltage is used to control the functionality of the A/Ds. The GMX can also instruct the DSPs individually: to test the functionality of each Voodoo, to wait for a trigger and to acquire data; to load a new program into its memory and to execute it.

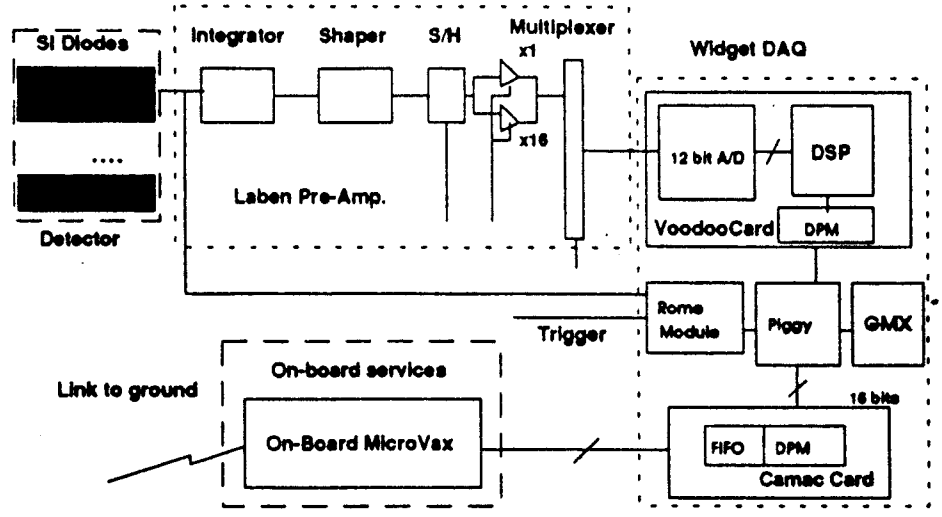

Fig. 2: The path followed by the signal for one data channel.

The PiggyBoard provides services such a nonvolatile memory used to store tables and programs, a watchdog reset system that - if not itself resetted by the GMX every second- generates a reset pulse for the whole system.

The RomeModule conditions the trigger into a TTL level. But its main function is to generate internally 10 Hz trigger pulses in order to calibrate the system. Under the command of the GMX it provides the preamplifiers with test-in levels, coming from a programmable D/A, to check the functionality and linearity of the pre-amplifiers. If the test-in voltage level is zero, Widget measures the noise of the system. The mean of the noise and the width of the its histogram determines the threshold. The determination of new thresholds can be achieved while flying, hence compensating for changes of the electronics, either intrinsic or produced by changes of environmental variables such as power supply noise or payload temperature.

The CamacBoard also allows the system to receive instructions from the ground. Consequently recalibrations and other tasks can be requested on demand, when some anomaly is noticed through the monitoring of the data arriving to the ground.

3. CONCLUSIONS

The flexibility and modularity of the system allows to accommodate from 1 to 20 planes with almost degradation of the acquisition data rate. The high programability permits, that with a simple change of software, novel tasks can be executed. Also, the presence of a general purpose computer allows the system to control the hardware faults minimizing their influence in the overall performance.

REFERENCES

[1] Wizard, v.1, Flight proposal in response to NASA A.O. NO. OSSA 3-88: 1988 Nov.
[2] Rancoita P. G.and Seidman A.:1982, La Riv. Nuo. Cim., 5, Series 3, #7.
[3] WIDGET: Hardware Technical Manual: 1993, Microprocessor Lab., ICTP, Trieste.
[4] WIDGET: Software User Manual: 1993, Microprocessor Lab., ICTP, Trieste.
[5] GMX Inc, "GMX Micro-20 68020 Single-board Computer";1992, Chicago.
[6] Texas Instruments, "TMS320C25 Digital Signal Processor, Product Description".
[7] Battaiotto P, Colavita A, Fratnik F, Lanceri L: 1991, Nucl. Instr. and Meth., A301, 265-268.